

Simple model of pion-nucleon elastic scattering

D. J. Ernst

Physics Department,* Texas A&M University, College Station, Texas 77843
and Physics Department,† University of Washington, Seattle, Washington 98195

Mikkel B. Johnson

Los Alamos Scientific Laboratory of the University of California, Los Alamos, New Mexico 87545

(Received 13 November 1979)

A nonstatic model for elastic pion-nucleon scattering is developed using knowledge of the analytic structure of the scattering amplitude and partial wave N/D dispersion techniques. In S , D , and F partial wave channels the model is equivalent to a separable potential model which includes the coupling to inelastic channels. In P -wave channels the nucleon pole which arises from absorption and emission of the pion is included. A more general model which incorporates both a nucleon pole term and a separable potential term is developed for the P_{11} channel. This model is capable of reproducing the change of sign which is present in the P_{11} phase shifts. The necessary information concerning the coupling of the inelastic scattering to the elastic scattering is taken from the experimentally determined phase shifts as input. If simple kinematic factors are included explicitly, quite simple analytic functions for the form factors in the model are able to reproduce the experimental phase shifts for pion laboratory kinetic energies up to 1.2 GeV. The model produces off-shell behavior which is different from previous models. In particular, the inclusion of the nucleon pole alters substantially the range of the interaction in all P -wave channels.

NUCLEAR REACTIONS Pion-nucleon elastic scattering; separable potential and Chew-Low models extended; S -, P -, D -, and F -wave phase shifts for $E \leq 1.2$ GeV.

I. INTRODUCTION

With the advent of pion beams at modern accelerators, there has arisen an interest in generating models of the pion-nucleon interaction at low energies. These models must be of a form that is suitable for use in theories of the pion-nucleus interaction. In order to do this, one must specify the off-shell as well as on-shell T matrices; one of the persistent ambiguities in pion physics seems to have been an understanding of this off-shell behavior. The question is especially relevant for making firm estimates of the size of higher order corrections to the optical potential.¹

One of the most popular models for the off-shell T matrix is based on the separable potential description.²⁻⁷ The first of these potentials⁵ was due to Landau and Tabakin and was generalized in Ref. 6 to include the coupling of the inelastic, pion production channels to the elastic channel. In Ref. 7 it was shown that the potential of Ref. 6 would arise from quite general assumptions concerning the underlying coupled channel interaction. The usefulness of these models is that they provide a unique relationship between the on-shell data (i.e., the phase shifts) and the off-shell extension of the T matrices.

A further question which one must ask is how adequate is the separable potential model. The study of approximating a given interaction by a separable interaction can shed considerable light

on this question. It has long been known that near a resonance, the T matrix is naturally separable. The separable T matrix can be explicitly constructed in terms of the wave functions of the Schrödinger equation with a complex energy.⁸ Away from resonance, short-range interactions are also well approximated by separable forms⁸ of low rank as long as the underlying Hamiltonian is energy independent. These studies can be used to justify the separable potential model in most of the partial wave channels.

In the P -wave channels, however, the pion-nucleon interaction is dominated by the repeated absorption and emission of the pion, as depicted in Fig. 1. This interaction is strongly energy dependent and *cannot* be approximated by a separable potential. A recent examination⁹ of the Chew-Low model¹⁰ has found that, if the coupling of the inelastic channels to the elastic channels^{9,11} is included in the model, then the Chew-Low model reproduces quite well⁹ the dominant P_{33} phase shifts over an extended energy range. The main mathematical difference between the Chew-Low model and the separable potential model can be

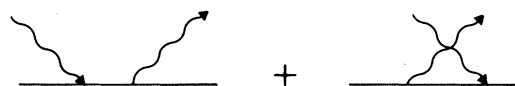


FIG. 1. The low orders graphs for pion absorption and emission which lead to the nucleon pole in the scattering amplitude.

easily seen if one examines the analytic structure of the T matrix $\langle \vec{k}' | T(z) | \vec{k} \rangle$ as a function of complex energy z . The Chew-Low model produces the analytic structure depicted in Fig. 2. The amplitude has the elastic scattering cut along the right-hand real axis, the inelastic scattering cuts also on the right-hand axis, the nucleon pole at the origin, and a left-hand cut which arises from crossing symmetry. The nucleon pole and crossing cut arise from the physical mechanism of absorption and creation of pions. The separable potential model T matrix possesses the elastic and inelastic cut but does not have the nucleon pole or the crossing cut. Since the nucleon pole lies only a pion mass below elastic threshold and dominates the low energy P -wave scattering, we feel that it is important that it be incorporated into the model. The role that this pole plays in the pion-nucleus problem has been examined by several authors.¹² Because the Chew-Low model is a dynamical model (the amplitude is derived from a Hamiltonian), how to continue the amplitude off-shell can be derived. A detailed examination of how we believe this amplitude is to be incorporated in the many-body problem is forthcoming.

In order to include the nuclear pole in the amplitude, but allow ourselves enough freedom to remain consistent with the data, we propose the following model. In partial waves other than P waves we use the separable potential model. In these waves, the contribution of the nucleon pole is quite small and our understanding of the underlying physics¹³ tells us that the interaction is short range and should, therefore, be well approximated by a separable potential. We do not use the inverse theory of Refs. 7 and 10 for several reasons. First, the inverse scattering theory requires that the pion-nucleon elastic scattering data be specified¹⁴ for all energies. Not only is this data not completely specified, but it is also not clear whether the model should be expected to be applicable for such a large range of energies. Second, generating the potential numerically from the data gives rise to inconvenient results. The results have no simple analytic form and also reflect the statistical fluctuations in the data. Third, once simple kinematic factors are included explicitly in the potentials, one finds that the phase shifts can be fit over a very large region by quite simple functions. In Sec. II we review the separable potential model

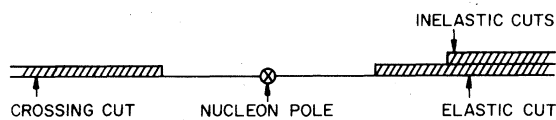


FIG. 2. The analytic structure of the scattering amplitude $\langle \vec{k}' | T(z) | \vec{k} \rangle$ as a function of complex z .

and present S -, D -, and F -wave potentials that reproduce the elastic scattering phase for $k_{c.m.} < 700$ MeV/c (or $T_{lab} < 1.2$ GeV).

In P -wave channels (other than the P_{11} channel) we use a Chew-Low type amplitude. We retain the nucleon pole in the model, but neglect the crossing cut. The inclusion of crossing symmetry requires the solution of nonlinear equations and would thus greatly complicate the model. Since crossing symmetry provides a non-negligible⁹ part of the interaction, we artificially account for its absence by an independent adjustment of the pion-nucleon coupling constant and form factor in each of the three channels P_{13} , P_{31} , and P_{33} . Results for these channels and details of the model are given in Sec. III.

The P_{11} channel presents its own special difficulties. The nucleon pole dominates at elastic scattering threshold⁹ and thus any model with this pole will fit the scattering volume reasonably well. The amplitudes which result from a Chew-Low model do not at all behave like the measured phase shifts which change signs at low energies and then rise through a resonance. This change in sign of the P_{11} phase shifts has often^{5,6} been ignored. We propose a model in the P_{11} channel which is capable of fitting the measured phase shifts in detail. In Sec. IV, we develop a hybrid model which possesses a term with a nucleon pole and another term which behaves like a separable potential. This gives us the freedom to reproduce the change in sign of the P_{11} phase shifts and fit the data in detail.

Pion-nucleon scattering has also been considered recently by Liu and Shakin.¹⁵ They obtained results for S and P waves, and we have considered S , P , D , and F waves. The higher partial waves are needed for studies of pion-nucleus scattering at energies above the (3-3) resonance. The model we propose is similar to that of Liu and Shakin in that the pion-nucleon pole term is taken into account explicitly in both investigations, although we omit the (small) contribution in partial waves $l \neq 1$. In neither work is the crossing cut taken into account explicitly. Liu and Shakin account for this term phenomenologically by introducing a background term in their T matrix, whereas we account for it by a slight adjustment of the pion-nucleon coupling constant and form factor (as long as one is not too close to the crossing cut it may be well approximated by a pole). Because the pole term is included, both amplitudes provide an extrapolation into the subthreshold region.

Although the model presented here and in Ref. 15 is motivated by similar physical ideas, the procedure used by Liu and Shakin is somewhat more complicated than ours and does not completely

determine the fully off-shell T matrix. In Ref. 15 a background term is introduced into all S - and P -wave channels. In the P_{11} and P_{33} channels a separable potential model is introduced, in addition, to account for the resonant part of the amplitude, and inverse scattering theory is used to obtain the potential. The introduction of a potential to account for the P_{33} resonance ignores the intimate relation between this resonance and the nucleon pole term implied by field theoretic models.^{9, 10} The background term consists of the nucleon pole and a discrepancy term, which is fit to the data. The off-shell momentum dependence of the T matrix (in the discrepancy term) is not determined¹⁵ by their theory, and in this regard our model is more complete than that of Liu and Shakin.

II. SEPARABLE POTENTIAL MODEL AND RESULTS FOR S , D , AND F WAVES

In this section we review the rank one separable potential model of Ref. 7 which includes the coupling of the elastic channel to the inelastic channels. A review of this model has also been presented in Ref. 16. The elastic scattering T matrix is decomposed into its partial wave and isospin states according to

$$\langle \vec{k}' | T(\omega) | \vec{k} \rangle = \sum_{\alpha} \langle k' | t_{\alpha}(\omega) | k \rangle P_{\alpha}(\hat{k}', \hat{k}), \quad (2.1)$$

where α stands for the set of quantum numbers $[J, L, T]$ and P_{α} is an operator which projects on-

to the state α and which is normed by

$$\int P_{J, L, T}(\hat{k}', \hat{k}'') P_{J', L', T'}(\hat{k}'', \hat{k}) d\Omega_{\hat{k}''} \\ = P_{J, L, T}(\hat{k}', \hat{k}) \delta_{J'J} \delta_{L'L} \quad (2.2)$$

This is not the normalization used in Refs. 2-7, but is taken from Ref. 17. The relation of $t_{\alpha}(k) \equiv \langle k | t_{\alpha}(\omega_{\pi}) | k \rangle$ to the phase shifts is given by

$$t_{\alpha}(k) = -\frac{\hbar^2 \omega(k)}{\pi k \omega_{\pi}(k) \omega_N(k)} \left(\frac{\eta_{\alpha} \exp(2i\delta_{\alpha}) - 1}{2i} \right) \\ = -\frac{\hbar^2 \omega(k)}{\pi k \omega_{\pi}(k) \omega_N(k)} (\hat{\eta}_{\alpha} e^{i\hat{\delta}_{\alpha}} \sin \hat{\delta}_{\alpha}) \quad (2.3)$$

with the energies defined by

$$\omega_N(k) = (k^2 + m_N^2)^{1/2}, \quad \omega_{\pi}(k) = (k^2 + m_{\pi}^2)^{1/2},$$

and

$$\omega(k) = \omega_N(k) + \omega_{\pi}(k),$$

where \vec{k} is the pion momentum in the center-of-mass frame. The parameters $\hat{\eta}_{\alpha}$ and $\hat{\delta}_{\alpha}$ are more convenient for our purposes than the more often used parameters η_{α} and δ_{α} . The parameter $\hat{\eta}_{\alpha}$ is simply the ratio of the total elastic cross section in channel α to the total cross section in channel α .

The separable potential model of Ref. 7 assumes an interaction matrix in channel space which has the form

$$\langle k' | V_{\alpha} | k \rangle = \begin{pmatrix} \lambda_{11} \bar{v}_{\alpha}(k') V_{\alpha}(k) & \lambda_{12} \bar{v}_{\alpha}(k') W_{\alpha,2}(k) & \lambda_{13} \bar{v}_{\alpha}(k') W_{\alpha,3}(k) & \cdots \\ \lambda_{12}^* W_{\alpha,2}(k') \bar{v}_{\alpha}(k) & V_{\alpha}^{22}(k', k) & V_{\alpha}^{23}(k', k) & \cdots \\ \lambda_{13}^* W_{\alpha,3}(k') \bar{v}_{\alpha}(k) & V_{\alpha}^{23}(k', k)^{\dagger} & V_{\alpha}^{33}(k', k) & \cdots \\ \vdots & \vdots & \vdots & \vdots \\ \vdots & \vdots & \vdots & \vdots \end{pmatrix}. \quad (2.4)$$

The superscripts i stand for the channel, with $i \geq 2$ being inelastic channels whose exact nature need not be specified. The potentials $W_{\alpha,i}$ and $V_{\alpha}^{i,j}(k', k)$ are arbitrary. The usefulness of this model is that in the elastic channel the off-shell T matrix has a simple separable form, valid for positive energies

$$\langle k' | t_{\alpha}[\omega(k_0)] | k \rangle = \frac{\bar{v}_{\alpha}(k')}{\bar{v}_{\alpha}(k_0)} t_{\alpha}(k_0) \frac{\bar{v}_{\alpha}(k)}{\bar{v}_{\alpha}(k_0)}. \quad (2.5)$$

Rather than follow the derivation of Ref. 7, we

shall here derive the separable potential model results¹⁶ from a partial wave N/D dispersion theory argument. This approach greatly clarifies the relation between the separable potential and Chew-Low models and also provides additional justification for the model.

The partial wave amplitude t_{α} is broken into two parts by the expression

$$\langle k' | t_{\alpha}(\omega) | k \rangle = \frac{N_{k'k}^{\alpha}}{D_{\alpha}(\omega)}. \quad (2.6)$$

This expression also serves to extend the off-shell model to negative energies. The analytic structure of the T matrix is divided between N^α and D_α by assuming that the elastic and inelastic cuts are both contained in $D_\alpha(\omega)$ while *all* other singularities are contained in N^α . We parametrize N^α by

$$N_{kk}^\alpha = +[\bar{v}_\alpha(k)]^2, \quad (2.7)$$

where $\bar{v}(k)$ is the potential form factor in Eqs. (2.4) and (2.5).

The behavior near elastic scattering threshold requires that $\bar{v}_\alpha(k) \rightarrow \bar{k}^l$ for small values of k . Furthermore, the relation of the scattering amplitude t_α to an invariant amplitude \mathfrak{M}_α in the center-of-mass system, is given by¹⁸

$$\langle k' | t_\alpha(\omega) | k \rangle = \left[\frac{m_N^2}{4\omega_\pi(k)\omega_\pi(k')\omega_N(k)\omega_N(k')} \right]^{1/2} \times \langle k' | \mathfrak{M}_\alpha | k \rangle. \quad (2.8)$$

Therefore, near $k=0$, we expect t_α to behave like $[\omega_\pi(k)\omega_\pi(k')]^{-1/2}k^{2l}$ and $\bar{v}_\alpha(k)$ to behave like $\omega_\pi(k)^{-1/2}k^l$. We display these kinematic factors explicitly in our potential by writing

$$\bar{v}_\alpha^2(k) = \frac{k^{2l}}{\omega_\pi(k)} v_\alpha^2(k), \quad (2.9)$$

and parametrizing $v_\alpha^2(k)$.

The analytic structure of $D_\alpha(\omega)$ consists of a cut along the real axis from $\omega = m_n + m_\pi$ to $+\infty$. Cauchy's theorem implies that $D_\alpha(\omega)$ may be written as

$$D_\alpha(\omega) = D_\alpha(\infty) - \frac{1}{\pi} \int_{m_n+m_\pi}^{\infty} d\omega' \frac{\text{Im} D_\alpha(\omega')}{\omega - \omega' + i\eta}. \quad (2.10)$$

From Eqs. (2.3), (2.6), (2.7), and (2.9) we have

$$\text{Im} D_\alpha[\omega(k)] = \pi \left[\frac{k^{2l+1} v_\alpha^2(k)}{\omega_\pi(k)} \right] \left[\frac{\omega_\pi(k)\omega_N(k)}{\hbar^2 \omega(k)\hat{\eta}_\alpha(k)} \right]. \quad (2.11)$$

If we define $\lambda = D_\alpha^{-1}(\infty)$, we find upon substitution of Eq. (2.11) into (2.10),

$$D_\alpha(\omega) = \frac{1}{\lambda_\alpha} \left(1 - \lambda_\alpha \int_0^\infty k^2 dk \frac{v_\alpha^2(k) k^{2l}}{\omega_\pi(k)\hat{\eta}_\alpha(k)} \times \frac{1}{\omega - \omega(k) + i\eta} \right) \quad (2.12)$$

and

$$N_\alpha[\omega(k)] = \frac{k^{2l} v_\alpha^2(k)}{\omega_\pi(k)}. \quad (2.13)$$

Simple forms are chosen for $v_\alpha^2(k)$ and then used in Eqs. (2.6), (2.12), and (2.13) to fit the

elastic scattering phase shifts $\hat{\delta}_\alpha$, in the S_{11} , S_{31} , D_{13} , D_{15} , D_{33} , D_{35} , F_{15} , F_{17} , F_{35} , and F_{37} channels for pion laboratory kinetic energies below about 1.2 GeV. The resulting phases are depicted in Figs. 3–12, together with the data from Refs. 19–22. The forms chosen for $v_\alpha^2(k)$ are given in Table I. For other than the S waves, $v_\alpha(k)$ equal to a simple Gaussian was sufficient; for the S -wave channels a slightly more complicated function had to be used. As errors had not been assigned many of the experimental phase shifts to which we fit, the parameters were adjusted until we judged that a good fit had been obtained. This means that the error in our parameters cannot be determined quantitatively.

The values for $\hat{\eta}_\alpha(k)$ were taken as input from Ref. 19. In three channels, the D_{33} , F_{17} , and F_{35} , the $\hat{\eta}_\alpha(k)$ derived from the data of Ref. 19 was not a continuous function. In these channels, the coupling to the inelastic channel becomes very large while the phase δ_α is still very small. In this case, very small errors in δ_α and η_α can lead to enormous errors in $\hat{\delta}_\alpha$ and $\hat{\eta}_\alpha$. We have thus used a smooth and continuous function for $\hat{\eta}_\alpha(k)$ which was consistent with assuming an error of $\pm 1^\circ$ in $\delta_\alpha(k)$ and ± 0.03 in $\eta_\alpha(k)$. The $\hat{\eta}_\alpha(k)$ used in the F_{35} channel together with the $\hat{\eta}_\alpha(k)$ derived from the phase shifts of Ref. 19 are depicted in Fig. 13. One should also notice that the phase $\hat{\delta}_\alpha(k)$ in these three channels for values of k near the inelastic threshold is very poorly determined. This is evidenced by the fact that the $\hat{\delta}_\alpha(k)$ do not form a continuous curve. In our fitting process, we therefore ignore these few data.

In all cases, the $\hat{\eta}_\alpha(k)$ are known only up to $k_{c.m.} = 887 \text{ MeV}/c$. We have continued the $\hat{\eta}_\alpha(k)$ beyond

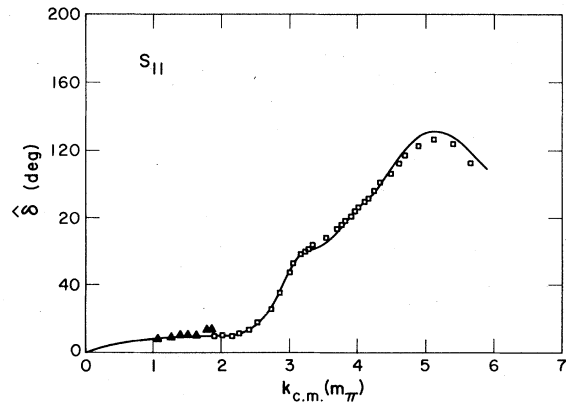


FIG. 3. The phase of the pion-nucleon scattering amplitude $\hat{\delta}$ in the S_{11} channel versus pion center-of-mass momentum. The curve is the prediction of the potential given in Table I. The open squares (\square) are the data from Ref. 19, and the solid triangles (\blacktriangle) are data from Ref. 21.

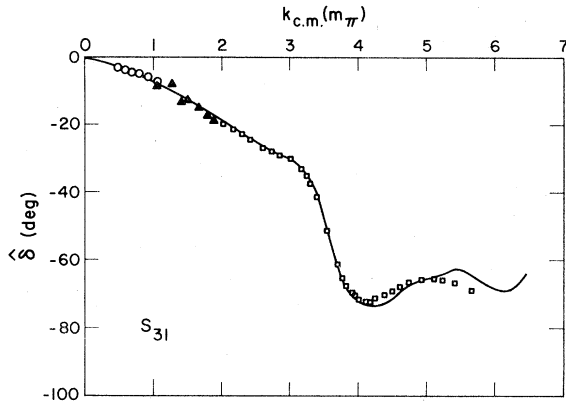


FIG. 4. The same as Fig. 3 except the S_{13} channel is presented. The open circles (O) are data from Ref. 22.

this point by bringing $\hat{\eta}_\alpha(k)$ back to unity¹⁴ by $k_{c.m.} = 1200$ MeV/c. This is also depicted for the F_{35} channel in Fig. 13.

The separable potential model which includes the coupling to the inelastic channels is able to produce phases δ_α (the phase of the S matrix) which pass through zero in some cases, as has been discussed at length in Ref. 7. The normal rank one separable potential which ignores the coupling to inelastic channels is not able to produce phases which change sign. In channels D_{15} , D_{33} , F_{17} , F_{35} , and F_{37} , the phase δ_α changes sign and thus we are only able to reproduce these phases by using the coupled channel model.

There has recently been much interest in determining the range of the pi-nucleon interaction. It is important to note that the interaction enters differently²³ in a Klein-Gordon equation than in a relativistic Schrödinger equation. The form factors $v(k)$ which do not include the kinematic factors of $\omega_\pi(k)^{-1/2}$ are the appropriate form factors for a Klein-Gordon equation. The transformation to the

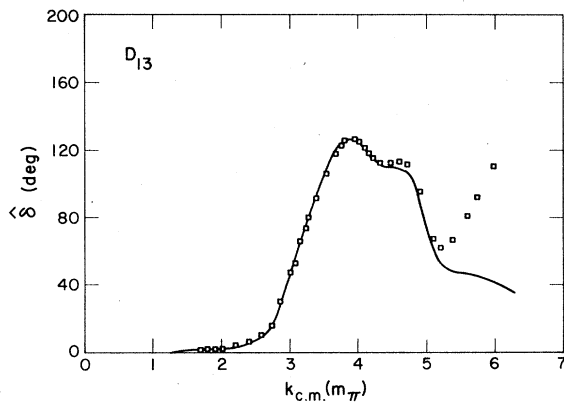


FIG. 5. The same as Fig. 3 except the D_{13} channel is presented.

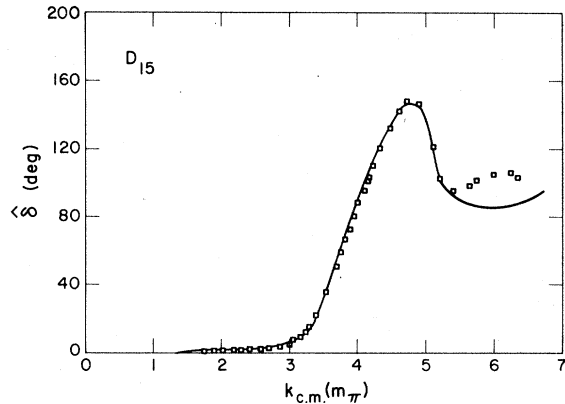


FIG. 6. The same as Fig. 3 except the D_{15} channel is presented.

relativistic Schrödinger equation brings in the factor of $\omega_\pi(k)^{-1/2}$. This factor has generally been included in the "form factor" implicitly.⁶ Its presence has often been overlooked, which has, in turn, led to some confusion in quoting ranges for form factors.

III. CHEW-LOW MODEL AND RESULTS FOR P_{13} , P_{31} , AND P_{33} CHANNELS

In the P_{13} , P_{31} , and P_{33} channels, we use a model based on the extended Chew-Low theory of Ref. 9. This model is similar to the separable potential model, with the important exception that it contains the nucleon pole term. We choose to neglect the crossing cut depicted in Fig. 1; we of course keep the lowest order crossed term depicted in Fig. 2. The inclusion of crossing symmetry requires the solution of nonlinear equations and would greatly complicate the model. Furthermore, the nonlinear, crossing symmetric Chew-Low equations have never been solved.^{9, 24} In order to fit the data

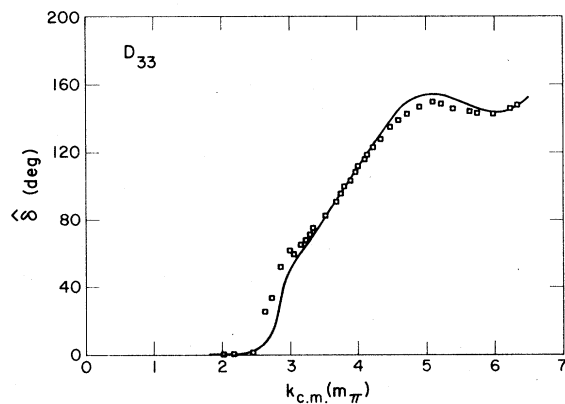


FIG. 7. The same as Fig. 3 except the D_{33} channel is presented.

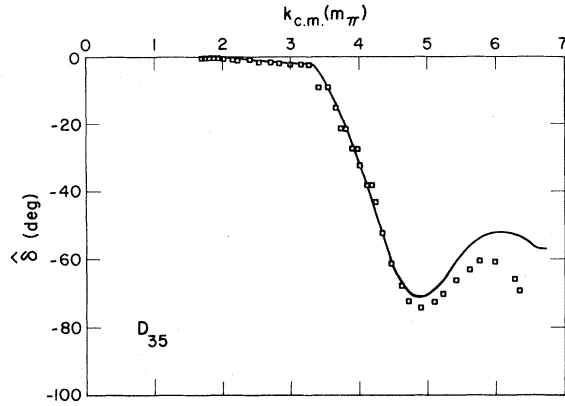


FIG. 8. The same as Fig. 3 except the D_{35} channel is presented.

in each of these three P -wave channels without crossing, we will have to vary the pion-nucleon coupling constant and form factor in each channel independently.

The crossed diagram in Fig. 2 is a u -channel pole in a relativistic theory. In the limit of infinite nucleon mass, this cannot be distinguished from an s -channel pole. We approximate the pole by its infinite mass form. Corrections to these approximations are small²⁵ for the purposes of our model. However, we do not take the nucleon mass to infinity in the Green's function appearing in $D(\omega)$ [see Eq. (3.5)], and we thereby avoid the static approximation of the Chew-Low theory. One consequence of this is that the unitarity condition [see Eq. (4.17)] possesses the proper kinetic factors.

We again break the amplitude into a numerator and denominator function. We shall assume that $D_\alpha(\omega)$ contains the nucleon pole, and the elastic and inelastic cuts; N^α will contain all other singularities. We again parametrize N^α by

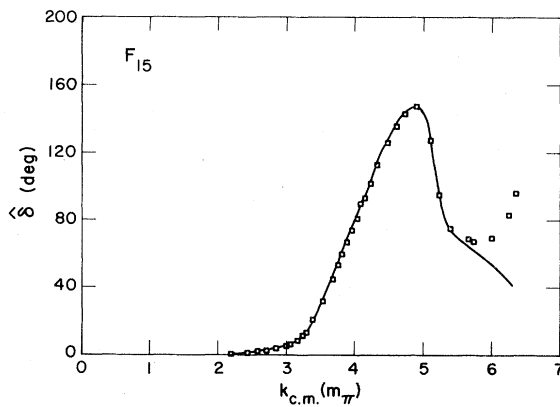


FIG. 9. The same as Fig. 3 except the F_{15} channel is presented.

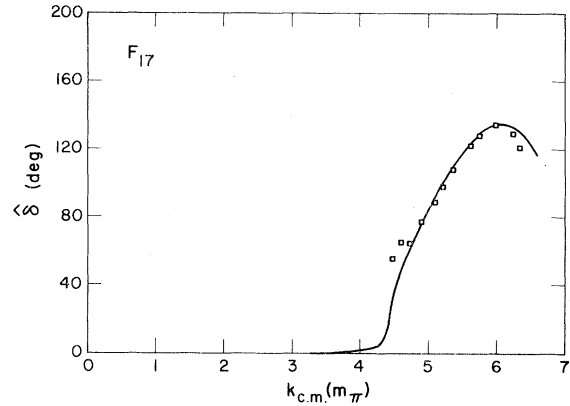


FIG. 10. The same as Fig. 3 except the F_{17} channel is presented.

$$N_{kk}^\alpha = \frac{k^2 v_\alpha^2(k)}{\omega_\pi(k)}, \quad (3.1)$$

where $v_\alpha^2(p)$ is the pion-nucleon form factor in the Chew-Low model. Cauchy's theorem for $D_\alpha(\omega)$ now implies

$$D_\alpha(\omega) = \omega_\pi \left[C_\alpha - \frac{1}{\pi} \int_{m_\pi + m_N}^{\infty} d\omega' \frac{\text{Im} D_\alpha(\omega') / \omega'_\pi}{\omega - \omega' + i\eta} \right], \quad (3.2)$$

where ω_π is (without an argument) related to ω by

$$\omega_\pi = (\omega^2 + m_\pi^2 - m_N^2) / 2\omega. \quad (3.3)$$

Using Eqs. (2.3), (2.6), and (3.1) we find

$$\text{Im} D_\alpha[\omega(k)] = \pi k \frac{v_\alpha^2(k) k^2}{\omega_\pi^2(k) \tilde{\eta}_\alpha(k)} \frac{\omega_\pi(k) \omega_N(k)}{\omega(k)}. \quad (3.4)$$

Substituting this into Eq. (3.2), defining $\lambda_\alpha = C_\alpha^{-1}$,

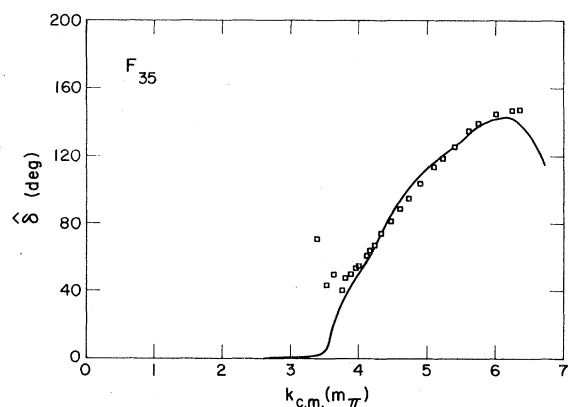


FIG. 11. The same as Fig. 3 except the F_{35} channel is presented.

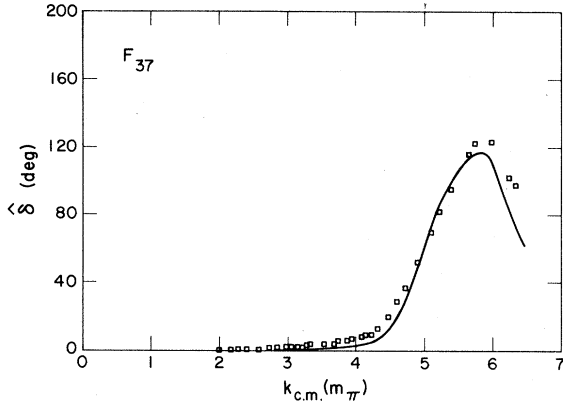


FIG. 12. The same as Fig. 3 except the F_{37} channel is presented.

we get

$$D_{\alpha}(\omega) = \frac{\omega_{\pi}}{\lambda_{\alpha}} \left[1 - \lambda_{\alpha} \int_0^{\infty} k'^2 dk' \frac{v_{\alpha}^2(k') k'^2}{\omega_{\pi}^2(k') \hat{\eta}_{\alpha}(k')} \times \frac{1}{\omega - \omega(k') + i\eta} \right]. \quad (3.5)$$

$$D_{\alpha}(\omega) = \omega_{\pi} \left[1 + \frac{\lambda_{\alpha}^{\text{CL}}(\omega - m_N)}{\pi} \int_0^{\infty} k'^2 dk' \frac{v_{\alpha}^2(k') k'^2}{\omega_{\pi}^2(k') \hat{\eta}_{\alpha}(k') [\omega(k') - m_N]} \frac{1}{\omega - \omega(k') + i\eta} \right]. \quad (3.9)$$

In the limit of infinite nucleon mass, Eqs. (3.8) and (3.9) are identically the Chew-Low expressions for the T matrix in the no-crossing approximations.

We parametrize $v_{\alpha}^2(k)$ according to Table II and fit the elastic phase shifts for $T_{\pi} \leq 1.2$ GeV as depicted in Figs. 14–16 for the P_{13} , P_{31} , and P_{33} channels.

This is the Chew-Low amplitude except for some corrections for the finite mass of the nucleon which occur naturally here.

We may rewrite Eqs. (3.4) and (3.5) in a more familiar form if we use

$$\frac{1}{\omega - \omega(k') + i\eta} = - \frac{1}{\omega(k') - m_N} + \frac{\omega - m_N}{\omega(k') - m_N} \frac{1}{\omega - \omega(k') + i\eta}, \quad (3.6)$$

and define the Chew-Low coupling constant $\lambda_{\alpha}^{\text{CL}}$ by

$$\frac{\lambda_{\alpha}^{\text{CL}}}{\pi} = -\lambda_{\alpha} \left[1 + \lambda_{\alpha} \int_0^{\infty} k'^2 dk' \times \frac{v_{\alpha}^2(k') k'^2}{\omega_{\pi}(k') \hat{\eta}_{\alpha}(k') [\omega(k') - m_N]} \right]^{-1}. \quad (3.7)$$

This gives the following expressions which are equivalent to Eqs. (3.4) and (3.5):

$$N_{\alpha k}^{\alpha} = \lambda_{\alpha}^{\text{CL}} \frac{k^2 v_{\alpha}^2(k)}{\pi \omega_{\pi}(k)} \quad (3.8)$$

and

In the dominant P_{33} channel we find a range for $v(p)$ of the order of 978 MeV/c. This is a number that is somewhat larger than was found in the full crossing symmetric Chew-Low model of Ref. 9. It should *not* be compared with the range of separable potential form factors which fit the same data. It was shown in Ref. 9 [Eq. (A15)] that a separable potential form factor which will identi-

TABLE I. The separable potential form factors and coupling constants defined in Eqs. (2.9), (2.12), and (2.13).

Channel	$v^2(k)$	λ_{α}	$\alpha_1(m_{\pi})$	A_2	$\alpha_2(m_{\pi})$
S_{11}	$\exp(-k^2/\alpha_1^2) + A_2 k^2 \exp(-k^2/\alpha_2^2)$	$-1.40 \times 10^{-2} m_{\pi}^{-1}$	1.612	$0.04865 m_{\pi}^{-2}$	16.12
S_{31}	$\exp(-k^2/\alpha_1^2) (1 + A_2 k^2)$	$+8.082 \times 10^{-2} m_{\pi}^{-1}$	3.247	$0.4053 m_{\pi}^{-2}$	
D_{13}	$\exp(-k^2/\alpha_1^2)$	$-2.138 \times 10^{-4} m_{\pi}^{-5}$	4.119		
D_{15}	$\exp(-k^2/\alpha_1^2)$	$-1.465 \times 10^{-5} m_{\pi}^{-5}$	10.12		
D_{33}	$\exp(-k^2/\alpha_1^2)$	$-4.061 \times 10^{-6} m_{\pi}^{-5}$	14.33		
D_{35}	$\exp(-k^2/\alpha_1^2)$	$+2.103 \times 10^{-4} m_{\pi}^{-5}$	3.582		
F_{15}	$\exp(-k^2/\alpha_1^2)$	$-1.207 \times 10^{-5} m_{\pi}^{-7}$	3.582		
F_{17}	$\exp(-k^2/\alpha_1^2)$	$-1.272 \times 10^{-7} m_{\pi}^{-7}$	8.954		
F_{35}	$\exp(-k^2/\alpha_1^2)$	$-2.503 \times 10^{-7} m_{\pi}^{-7}$	8.066		
F_{37}	$\exp(-k^2/\alpha_1^2)$	$-6.897 \times 10^{-7} m_{\pi}^{-7}$	6.447		

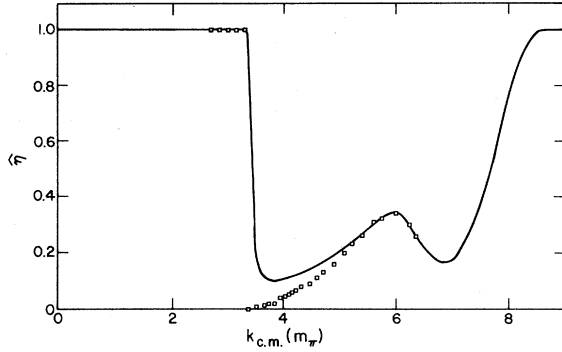


FIG. 13. The inelasticity parameter $\hat{\eta}(k)$ in the F_{35} channel vs pion center-of-mass momentum. The curve represents the smooth function used in the calculations while the squares represent the data from Ref. 19.

cally reproduce the phases predicted by a Chew-Low model is

$$\bar{v}_{\alpha}(k) = \frac{v_{\alpha}^{\text{CL}}(k)k}{\omega_{\pi}(k)}. \quad (3.10)$$

The factor of $\omega_{\pi}(k)$ in the denominator necessarily gives a longer range (in coordinate space) behavior to the separable potential.

The Chew-Low coupling constants as defined in Eq. (3.7) have also been calculated. We define $\lambda_{\alpha}^{\text{CL}} = \frac{2}{3} 1/m_{\pi}^2 f_{\alpha}^2(-4, -1, 2)$ for $\alpha = P_{11}, P_{13}$ and P_{31}, P_{33} , respectively. We find $f_{\alpha}^2 = 0.0552, 0.133,$ and 0.114 for the $P_{13}, P_{31},$ and P_{33} channels. This is to be compared with $f^2 = 0.081$ for all channels in the Chew-Low model. The increase in the coupling constant in the P_{33} channel is a compensation for neglecting crossing. The Chew-Low model, once it is extended to include the inelastic cut as in Ref. 9, will reproduce the P_{33} phase shifts with $f^2 = 0.081$. In the P_{13} (P_{31}) channel, the Chew-Low theory with $f^2 = 0.081$ gives phase shifts which are too large (small). In order to fit the data, we have therefore had to decrease (increase) the coupling constant in this channel.

IV. P_{11} CHANNEL

The P_{11} channel presents its own particular set of difficulties. The first problem arises because the phase shifts pass through zero below inelastic

TABLE II. Chew-Low form factors and coupling constants as defined in Eqs. (3.4) and (3.5).

Channel	$v^2(k)$	λ_{α}	$\alpha_1(m_{\pi})$
P_{13}	$\exp(-k^2/\alpha_1^2)$	$+4.067 \times 10^{-2} m_{\pi}^{-2}$	10.16
P_{31}	$\exp(-k^2/\alpha_1^2)$	$+5.247 \times 10^{-2} m_{\pi}^{-2}$	6.447
P_{33}	$\exp(-k^2/\alpha_1^2)$	$-1.863 \times 10^{-2} m_{\pi}^{-2}$	4.956

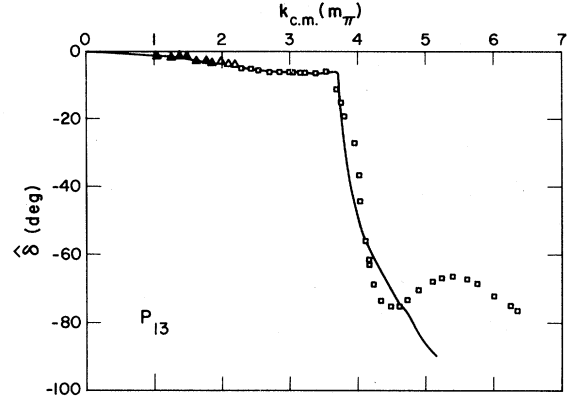


FIG. 14. The phase of the pion-nucleon scattering amplitude in the P_{13} channel versus pion center-of-mass momentum. The curve is predicted by our Chew-Low type model with the form factor given in Table II. The data is from Refs. 19, 21, and 22 as in Figs. 3-12 while the open triangles (Δ) are from Ref. 20.

threshold. Although the separable potential model of Ref. 7 can produce phase shifts, δ_{α} , which pass through zero in many cases, the particular behavior of the P_{11} phase shifts is beyond the model of Ref. 7. The second problem that arises in the P_{11} channel is that, in the Chew-Low model with crossing neglected, no canonical solution exists²⁶ for physically reasonable coupling constants. These solutions do not behave at all like the data. We are therefore forced to develop a new model for this channel.

The model we propose combines the separable potential model with the Chew-Low model. Since, near elastic threshold, the nucleon pole produces the correct scattering volume, we keep a term with the nucleon pole. In order for the phase shifts to change sign, we add a separable potential type term which dominates at high momentum (short range in coordinate space).

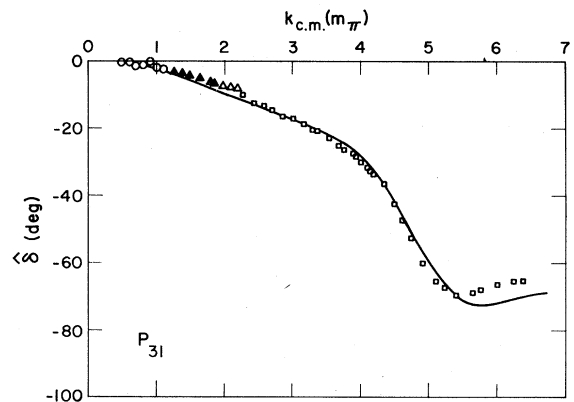


FIG. 15. The same as Fig. 14 except the P_{31} channel is presented.

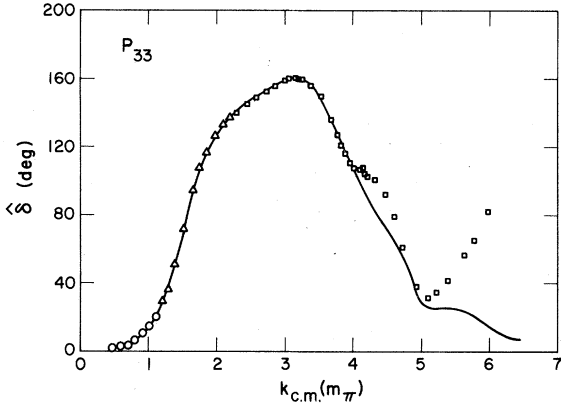


FIG. 16. The same as Fig. 14 except the P_{33} channel is presented.

We propose a form for the τ matrix in Eq.

$$\langle k | t_{\alpha}[\omega(k)] | k \rangle = [v_1(k)v_2(k)] \begin{bmatrix} \tau_{11} & \tau_{12} \\ \tau_{21} & \tau_{22} \end{bmatrix} \begin{bmatrix} v_1(k) \\ v_2(k) \end{bmatrix} \frac{k^2}{\omega_{\pi}(k)}, \quad (4.1)$$

where we have written t_{α} in terms of matrix multiplication for convenience. The quantity which is analogous to the denominator function in the previous models is the inverse of the τ matrix in Eq. (4.1). We call this inverse D ,

$$\sum_j \tau_{ij} D_{jk} = \delta_{ik}. \quad (4.2)$$

In terms of the matrix D , the scattering matrix t_{α} may be written

$$\langle k | t_{\alpha}[\omega(k)] | k \rangle = [v_1(k)v_2(k)] \frac{\begin{pmatrix} D_{22} & -D_{12} \\ -D_{21} & D_{11} \end{pmatrix}}{\mathfrak{D}} \begin{bmatrix} v_1(k) \\ v_2(k) \end{bmatrix} \frac{k^2}{\omega_{\pi}(k)}. \quad (4.3)$$

This expression replaces the division of t_{α} into N^{α} and D_{α} . The determinant of D is called \mathfrak{D} and is given by

$$\mathfrak{D} = D_{11}D_{22} - D_{12}D_{21}. \quad (4.4)$$

We now make the following assumptions concerning the analytic structure of the elements of D . The nucleon pole and the elastic and inelastic cuts are contained in D , while all other singularities will be incorporated into the factors $v_i(k)$. We will incorporate the nucleon pole into D_{11} . If in the limit $v_2(k) \rightarrow 0$ we require that we recover our previous Chew-Low⁹ results, we have

$$D_{11}(\omega) = \frac{\omega_{\pi}}{\lambda_{11}} \left(1 - \lambda_{11} \int_0^{\infty} k'^2 dk' \frac{v_1^2(k')k'^2}{\omega_{\pi}^2(k')\bar{\eta}_{11}(k')} \times \frac{1}{\omega - \omega(k') + i\eta} \right), \quad (4.5)$$

where $\bar{\eta}_{11}$ is the inelastic parameter which would result if $v_2(k)$ were zero. Similarly, we require that we recover our previous separable potential result in the limit $v_1(k) \rightarrow 0$ to obtain

$$D_{22}(\omega) = \frac{1}{\lambda_{22}} \left(1 - \lambda_{22} \int_0^{\infty} k'^2 dk' \frac{v_2^2(k')k'^2}{\omega_{\pi}(k')\bar{\eta}_{22}(k')} \times \frac{1}{\omega - \omega(k') + i\eta} \right), \quad (4.6)$$

where again $\bar{\eta}_{22}$ is the inelastic parameter which would result if v_1 were zero. We also assume that $D_{12} = D_{21}$.

Near the nucleon pole ($\omega_{\pi} \rightarrow 0$), our amplitude becomes

$$\langle k | t_{\alpha}[\omega(k)] | k \rangle = \frac{1}{\omega_{\pi}(k)\bar{D}_{11}D_{22} - D_{12}^2} [v_1(k)v_2(k)] \times \begin{bmatrix} D_{22} & -D_{12} \\ -D_{12} & 0 \end{bmatrix} \begin{bmatrix} v_1(k) \\ v_2(k) \end{bmatrix} \frac{k^2}{\omega_{\pi}(k)}, \quad (4.7)$$

where $\bar{D}_{11}(\omega) = \omega_{\pi}^{-1}D_{11}(\omega)$. If we are going to have a pole, D_{12}^2 must approach zero faster than ω_{π} . We require

$$\lim_{\omega_{\pi} \rightarrow 0} D_{12}(\omega) \rightarrow \omega_{\pi}\bar{D}_{12}(\omega). \quad (4.8)$$

In this case we have

$$\lim_{\omega_{\pi} \rightarrow 0} \langle k | T[\omega(k)] | k \rangle \rightarrow \frac{v_1^2(k)k^2/\omega_{\pi}(k)}{\omega_{\pi}(k)\bar{D}_{11}(\omega)} \quad (4.9)$$

and the behavior of the amplitude near the pole becomes independent of $v_2(k)$.

The function $D_{12}(\omega)$ can at most contain the elastic and inelastic cut. This, together with Eq. (4.9), allows us to write

$$D_{12}(\omega) = \omega_{\pi} \left(C_{12} - \frac{1}{\pi} \int_{m_{\pi} + m_N}^{\infty} d\omega' \frac{\text{Im}D_{12}(\omega')/\omega'_{\pi}}{\omega - \omega' + i\eta} \right). \quad (4.10)$$

For convenience we parametrize $\text{Im}D_{12}$ by

$$\text{Im}D_{12}[\omega(k)] = \frac{\pi v_1(k)v_2(k)k^3\omega_{\pi}(k)}{\bar{\eta}_{12}(k)\omega(k)}, \quad (4.11)$$

so that Eq. (4.10) becomes

$$D_{12}(\omega) = \omega_{\pi} \left[C_{12} - \int_0^{\infty} k'^2 dk' \frac{v_1(k')v_2(k')k'^2}{\omega_{\pi}^2(k')\bar{\eta}_{12}(k')} \times \frac{1}{\omega - \omega(k') + i\eta} \right]. \quad (4.12)$$

The function $\bar{\eta}_{12}(k)$ does not seem to have any simple physical interpretation; it is merely a

convenient way of parametrizing $\text{Im}D[\omega(k)]$.

The constant C_{12} determines the behavior of the model at high energy. We have

$$\lim_{\omega(k) \rightarrow \infty} \langle k | t_\alpha[\omega(k)] | k \rangle \rightarrow \frac{\lambda_{22}[v_2^2(k) - 2\lambda_{11}v_1(k)v_2(k)C_{12}]}{1 - \lambda_{11}\lambda_{12}C_{12}^2\omega_\pi(k)} \times \frac{k^2}{\omega_\pi(k)}. \quad (4.13)$$

We choose C_{12} to be zero; the model then goes over to the Born approximation for $v_2(k)$ in the limit of high energy.

This is as far as we can proceed without a dynamic model of the inelastic channels or making further assumptions. We do not have experimental results to determine $\bar{\eta}_{11}$, $\bar{\eta}_{22}$, or $\bar{\eta}_{12}$. Instead, we have the five functions $v_1(k)$, $v_2(k)$, $\bar{\eta}_{11}(k)$, $\bar{\eta}_{22}(k)$, and $\bar{\eta}_{12}(k)$. In the rank one case, we were able to use data to determine the necessary con-

tribution of the inelastic cut.

For simplicity we assume that all the $\bar{\eta}$'s are equal,

$$\bar{\eta}_{11}(k) = \bar{\eta}_{22}(k) = \bar{\eta}_{12}(k) = \hat{\eta}(k). \quad (4.14)$$

That this assumption is consistent with unitarity follows from the following argument. The unitarity condition is conveniently expressed in terms of the function \mathfrak{X} defined by

$$\mathfrak{X}[\omega(k)] \equiv [v_1(k)v_2(k)] \begin{pmatrix} D_{22} & -D_{12} \\ -D_{12} & D_{11} \end{pmatrix} \begin{pmatrix} v_1(k) \\ v_2(k) \end{pmatrix} \frac{k^2}{\omega_\pi(k)}. \quad (4.15)$$

The relation, Eq. (4.14), makes \mathfrak{X} real as can be seen from

$$\begin{aligned} \text{Im} \mathfrak{X}[\omega(k)] &= \frac{k^2}{\omega_\pi(k)} [v_1^2(k)\text{Im}D_{22} + v_2^2(k)\text{Im}D_{11} - 2v_1(k)v_2(k)\text{Im}D_{12}] \\ &= \frac{k^5\pi\omega_N(k)}{\omega(k)} \left[v_1^2(k) \frac{v_2^2(k)}{\bar{\eta}_{22}(k)} + v_2^2(k) \frac{v_1^2(k)}{\bar{\eta}_{11}(k)} - 2v_1(k)v_2(k) \frac{v_1(k)v_2(k)}{\bar{\eta}_{12}(k)} \right] \\ &= \frac{\pi k^5\omega_N(k)v_1^2(k)v_2^2(k)}{\omega(k)} \left[\frac{1}{\bar{\eta}_{22}(k)} + \frac{1}{\bar{\eta}_{11}(k)} - \frac{2}{\bar{\eta}_{12}(k)} \right] = 0. \end{aligned} \quad (4.16)$$

The unitarity condition follows immediately from Eq. (2.3). It states

$$|t_\alpha[\omega(k)]|^2 = - \frac{\hat{\eta}^2\omega(k)}{\pi k\omega_\pi(k)\omega_N(k)} \hat{\eta}_\alpha(k)\text{Im}t_\alpha[\omega(k)]. \quad (4.17)$$

This gives for $t_\alpha(k)$, as parametrized in Eq. (4.3) and (4.15),

$$\begin{aligned} |\mathfrak{X}[\omega(k)]|^2 &= - \frac{\omega(k)}{\pi k\omega_\pi(k)\omega_N(k)} \hat{\eta}_\alpha(k)\text{Im}\{\mathfrak{X}[\omega(k)]\mathfrak{D}^*[\omega(k)]\}. \end{aligned} \quad (4.18)$$

This becomes for \mathfrak{X} real

$$\mathfrak{X}[\omega(k)] = \frac{\omega(k)}{\pi k\omega_\pi(k)\omega_N(k)} \hat{\eta} \text{Im} \mathfrak{D}[\omega(k)]. \quad (4.19)$$

The imaginary part of \mathfrak{D} is given by

$$\begin{aligned} \text{Im} \mathfrak{D} &= \text{Re}D_{11}\text{Im}D_{12} + \text{Re}D_{22}\text{Im}D_{11} - 2\text{Re}D_{12}\text{Im}D_{12} \\ &= \frac{k^3\pi\omega_N(k)}{\omega(k)\hat{\eta}(k)} \{v_2^2(k)\text{Re}D_{11} + v_1^2(k)\text{Re}D_{22} \\ &\quad - 2v_1(k)v_2(k)\text{Re}D_{12}\}. \end{aligned} \quad (4.20)$$

Substituting this into the right-hand side of Eq. (4.19) immediately reproduces the definition of \mathfrak{X} ,

Eq. (4.15). Thus, the choice of taking all the $\bar{\eta}$'s to be equal to the physical $\hat{\eta}(k)$ is a simple and consistent way of ensuring that the model will reproduce the experimental inelasticities.

We have adjusted λ_{11} , λ_{12} , $v_1(k)$, and $v_2(k)$ to fit the experimental phase shifts. The results are shown in Fig. 17 and the values of the parameters

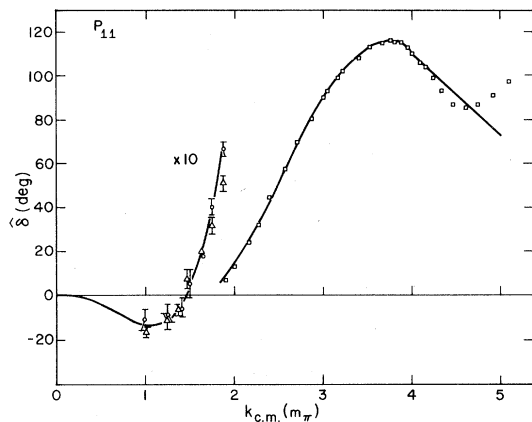


FIG. 17. The same as Fig. 14 except the P_{11} channel is presented. The form factors are given in Table III. Notice that for small k the graph and the data have been multiplied by 10 to better show the quality of the fit.

are given in Table III. In order that this model may readily be used by others, we have generated a simple fit to $\text{Re}D_{ij}[\omega(k)]$; the forms and results of this fit are given in the Appendix.

We have used Eq. (3.7) to generate an effective Chew-Low coupling constant in the P_{11} channel. We find $\lambda_{\alpha}^{\text{CL}} = (-\frac{8}{3})m_{\pi}^{-2}f_{\alpha}^{-2}$ with $f_{\alpha}^2 = 0.0369$ compared with the Chew-Low value of 0.081. There is one thing that is surprising about this result. We have found the P_{13} , P_{31} , and P_{33} channels to be reasonably consistent with the Chew-Low model in that the coupling constants are reasonably close to the value of 0.081 and that the form factors have consistently large cutoff values. However, in the P_{11} channel, the Chew-Low form factor $[v_1(k)]$ cuts off very rapidly in momentum. We have tried to reproduce the phases with a large cutoff in $v_1(k)$ but were unable to accomplish this.

V. CONCLUSIONS

We have derived a model which in channels other than the P -wave channels is equivalent to the separable potential model of Ref. 7. In these channels the interaction is believed to be dominated by the exchange of heavy mesons.¹³ This type of interaction leads to energy independent²⁷ potentials which are well approximated by a separable form.⁸ In the P -wave channels we are guided by the Chew-Low model and include the nucleon-pole term. In all cases the coupling of the inelastic channels to the elastic channel is included. In the P_{11} channel we develop a rank two N/D model with a low energy term that contains the nucleon pole and a high energy term that is like a separable potential in character. In all channels, we are able to fit the measured pion-nucleon phases for $T_{\pi} \lesssim 1.2$ GeV.

We have not addressed ourselves explicitly to the question of how this interaction should be incorporated into a multiple scattering type framework for pion-nucleus scattering. This is a question which is under investigation. It is important to notice that the off-shell behavior of the two-body amplitude is related to which relativistic equation²³ one is using. If one uses the Klein-Gordon equation, then presumably the short-range factors $v(k)$ listed in Tables I-III are the appropriate off-shell extrapolation factors. This would then imply

TABLE III. The form factors and coupling constants for the P_{11} interaction in Eqs. (4.3), (4.5), (4.6), and (4.12).

Form factor	Form	λ_i	$\alpha_i(m_{\pi})$
$v_1^2(k)$	$\exp(-k^2/\alpha_1^2)$	$0.032m^{-2}$	1.612
$v_2^2(k)$	$\exp(-k^2/\alpha_1^2)$	$-0.00212m_{\pi}^{-3}$	9.312

that the appropriate factors to use in a relativistic Schrödinger equation would be $v(k)/\omega_{\pi}(k)^{1/2}$. If one uses the propagator of Miller,¹² additional factors of $\omega_{\pi}(k)$ will be introduced.

We have neglected crossing symmetry. The role of crossing symmetry in the two-body problem is not clear because the crossing symmetric equations have never been solved. The approximate solutions of Refs. 9 and 24 indicate that crossing symmetry provides a substantial contribution. The role of crossing symmetry in the many-body problem has been examined by Cammarata and Banerjee.¹²

The off-shell behavior of the model proposed here is substantially different from the separable potential models in all the partial wave channels. Our off-shell extension is much smoother than that of Ref. 6 because we fit only the experimental phases which exist for laboratory kinetic energies below 1.2 GeV. The inclusion of the nucleon pole changes the range of the off-shell factors in the P -wave channels. In the P_{11} channel, we have not only included the nucleon pole, but have also produced a model which is capable of reproducing the change in sign of the experimental phase shifts. For $k \lesssim 2$ m, the off-shell behavior of this model is totally different from the potential models^{5,6} which represent an everywhere attractive interaction. Methods for incorporating this interaction into the many-body problem and its implications for elastic and inelastic pion-nucleus scattering are under investigation.

ACKNOWLEDGMENTS

The work of D. J. E. was supported in part by the National Science Foundation and the Department of Energy. The work of M. J. B. was performed under the auspices of the U. S. Department of Energy.

APPENDIX

In this appendix we present analytical forms for the real part of the functions D_{11} , D_{12} , and D_{22} defined in Eqs. (4.5), (4.6), and (4.2). These forms then allow one to continue the model off-shell without having to recalculate the principle value integrations involved in the definitions of the functions.

First, we define functions which remove the explicit dependence of the D_{ij} on ω ,

$$\text{Re}D_{12}(\omega) = \frac{\omega\pi}{\lambda_{11}} g_{11}(\omega), \quad (\text{A1})$$

$$\text{Re}D_{12}(\omega) = \omega_{\pi} m_{\pi}^2 g_{12}(\omega), \quad (\text{A2})$$

and

TABLE IV. The expansion parameters A^{ij} defined in Eq. (A4). Each expansion is valid for $g_{ij}[\omega(k)]$ for $k_{\min} \leq k \leq k_{\max}$.

	k_{\min} (MeV/c)	k_{\max} (MeV/c)	k_0 (MeV/c)	A_0^{ij}	A_1^{ij}	A_2^{ij}	A_3^{ij}	A_4^{ij}
$g_{11}(\omega)$	0	800	400	0.9615	-0.0325	0.0554	0.0049	-0.0011
$g_{12}(\omega)$	0	240	120	4.0995	0.3128	-0.3098	-0.0502	0.0317
	240	320	280	3.6486	-0.2452	-0.4263	-0.0453	0.0497
	320	480	400	-0.6640	-0.8193	0.1978	-0.0115	0.0018
	480	800	640	-3.0810	-0.1654	0.7087	0.0207	-0.093
$g_{22}(\omega)$	0	400	200	0.2444	-0.0927	-0.0238	0.0036	0.0020
	400	800	600	-0.1528	0.2478	0.2424	0.0271	0.0321

$$\text{Re}D_{22}(\omega) = \frac{1}{\lambda_{22}} g_{22}(\omega). \quad (\text{A3})$$

$$s(\omega) = \frac{k(\omega) - k_0}{\Delta}, \quad (\text{A5})$$

We then fit polynomials to the functions $g_{ij}(\omega)$. These functions, particularly $g_{12}(\omega)$, have considerable structure so we fit it with different polynomials over different regions of energy.

We expand $g_{ij}(\omega)$ by

$$g_{ij}(\omega) = \sum_{\alpha=0}^4 A_{\alpha}^{ij} s(\omega)^{\alpha} \quad (\text{A4})$$

with $s(\omega)$ given by

where $k(\omega)$ is the momentum which corresponds to the total center-of-mass energy $\omega(k)$. The coefficients of this expansion A^{ij} , the parameter k_0 in Eq. (A5), and the region $k_{\min} \leq k \leq k_{\max}$, over which the expansion is valid, are given in Table IV. The parameter Δ in Eq. (A5) is given by

$$\Delta = \frac{1}{2} (k_{\max} - k_0). \quad (\text{A6})$$

*On leave.

†Present address.

¹H. Garcilazo, Nucl. Phys. A302, 493 (1978); J. M. Eisenberg, J. Hufner, and E. J. Moniz, Phys. Lett. B47, 381 (1973); M. B. Johnson and B. D. Keister, Nucl. Phys. A305, 461 (1978).

²R. H. Landau, S. C. Phatak, and F. Tabakin, Ann. Phys. (N.Y.) 78, 299 (1973); S. C. Phatak, F. Tabakin, and R. H. Landau, Phys. Rev. C 6, 1804 (1973); R. H. Landau, Ann. Phys. (N.Y.) 92, 205 (1975); Phys. Lett. 57B, 13 (1975); Phys. Rev. C 15, 2127 (1977).

³M. G. Piepho and G. E. Walker, Phys. Rev. C 9, 1352 (1974); E. R. Siciliano and G. E. Walker, *ibid.* 13, 257 (1976); W. R. Gibbs, B. F. Gibson, A. I. Hess, G. J. Stephenson, Jr., and W. B. Kaufman, *ibid.* 13, 2433 (1976); A. T. Hess and B. F. Gibson, *ibid.* 13, 749 (1976); L. S. Celenza, M. K. Liou, L. C. Liu, and C. M. Shakin, *ibid.* 10, 398 (1974); 10, 435 (1974); L. Celenza, L. C. Liu, and C. M. Shakin, *ibid.* 11, 1593 (1975); 12, 721 (1975); 12, 1983 (1975); 13, 2451 (1976); L. C. Liu and C. M. Shakin, *ibid.* 16, 333 (1978); 16, 1963 (1978); L. C. Liu, *ibid.* 17, 1787 (1978); K. Schwarz, H. F. K. Zingle, and L. Mathe-litsch, Phys. Lett. 83B, 297 (1979).

⁴R. H. Landau and A. W. Thomas, Phys. Lett. 41B, 361 (1976); Nucl. Phys. A302, 461 (1978).

⁵R. H. Landau and F. Tabakin, Phys. Rev. D 5, 2746 (1972).

⁶J. T. Londergan, K. W. McVoy, and E. J. Moniz, Ann. Phys. (N.Y.) 86, 147 (1974).

⁷D. J. Ernst, J. T. Londergan, E. J. Moniz, and R. M. Thaler, Phys. Rev. C 10, 1708 (1974).

⁸R. C. Fuller, Phys. Rev. 188, 1649 (1969); S. K. Adhikari, Phys. Rev. C 10, 1623 (1974); S. K. Adhikari and I. H. Sloan, *ibid.* 11, 1133 (1975); D. J. Ernst, C. M. Shakin, and R. M. Thaler, *ibid.* 8, 46 (1973); 9, 1780 (1974); D. J. Ernst, C. M. Shakin, R. M. Thaler, and D. L. Weiss, *ibid.* 8, 2056 (1973); R. J. McLeod and D. J. Ernst, *ibid.* 18, 1060 (1978); S. Peiper, *ibid.* 9, 883 (1974).

⁹D. J. Ernst and M. B. Johnson, Phys. Rev. C 17, 247 (1978).

¹⁰G. F. Chew and F. E. Low, Phys. Rev. 101, 1570 (1956); F. E. Low, *ibid.* 97, 1392 (1965).

¹¹C. B. Dover, D. J. Ernst, R. A. Friedenber, and R. M. Thaler, Phys. Rev. Lett. 33, 728 (1974); K. K. Bajaj and Y. Nogami, *ibid.* 34, 701 (1975).

¹²I. R. Afnan and B. Blankleider, report (unpublished); F. Myrer and A. W. Thomas, Nucl. Phys. A326, 497 (1979); A. S. Rinat, *ibid.* A287, 399 (1977); T. Mitzutani and D. S. Koltun, Ann. Phys. (N.Y.) 109, 1 (1977); I. R. Afnan and A. W. Thomas, Phys. Rev. C 10, 109 (1974); G. A. Miller, *ibid.* 16, 2325 (1977); J. B. Cammarata and M. K. Banerjee, *ibid.* 13, 299 (1976).

¹³M. G. Olsson and E. J. Osypowski, Nucl. Phys. B101, 136 (1975); R. Hackman, Phys. Rev. D 8, 3920 (1973); M. D. Seadron, in *Few Body Dynamics*, edited by A. N. Mitra, I. Slaus, V. S. Bhaim, and V. K. Gupta (North-Holland, Amsterdam, 1976).

¹⁴Different treatments of the high energy phase shifts can produce very different form factors as has been shown by D. J. Ernst and G. A. Miller, Phys. Rev. C 12, 1962 (1975).

- ¹⁵L. C. Liu and C. M. Shakin, *Phys. Rev. C* 18, 604 (1978).
- ¹⁶D. J. Ernst, *Interactions of Pions with Nucleons at Low Energies* (C. I. E. A. del I. P. N., Mexico, 1976).
- ¹⁷M. L. Goldberger and K. M. Watson, *Collision Theory* (Wiley, New York, 1964).
- ¹⁸J. D. Bjorken and S. D. Drell, *Relativistic Quantum Mechanics* (McGraw-Hill, New York, 1964).
- ¹⁹D. J. Herndon, A. Barbaro-Galtieri, and A. H. Rosenfeld, Lawrence Radiation Laboratory Report No. UCLR-20030, 1970 (unpublished). CERN theoretical phase shifts are used for $p \geq 2m_\pi$; below this, the more recent data of Refs. 20-32 are used.
- ²⁰J. R. Carter, D. V. Rugg, and A. A. Carter, *Nucl. Phys. B* 58, 378 (1973).
- ²¹H. Zimmerman, *Helv. Phys. Acta* 48, 191 (1975).
- ²²P. Y. Bertin, B. Coupat, A. Hivernat, D. B. Isabelle, J. Duclos, A. Gerard, J. Miller, J. Morgenstern, J. Picard, P. Vernin, and R. Powers, *Nucl. Phys. B* 106, 341 (1976).
- ²³M. B. Johnson and D. J. Ernst, *Phys. Rev. C* 20, 1064 (1979).
- ²⁴G. Salzman and F. Salzman, *Phys. Rev.* 108, 1619 (1957).
- ²⁵R. J. McLeod and D. J. Ernst (unpublished).
- ²⁶D. J. Ernst, R. A. Friedenber, and M. B. Johnson, *Z. Phys. A* 287, 363 (1978). The assertion that the addition of a CDD pole could produce a solution has been shown not to hold (private communication, Y. Nogami).
- ²⁷M. B. Johnson, *Ann. Phys. (N.Y.)* 97, 400 (1976).